

# Development of four-dimensional imaging spectrometers (4D-IS)

Nahum Gat, Gordon Scriven, John Garman, Ming De Li, Jingyi Zhang  
Opto-Knowledge Systems, Inc. (OKSI)

## ABSTRACT

The incentive for the 4D-IS concept was driven by the need to adequately resolve all four dimensions of data (2D spatial, spectral, and temporal) with a single, radiometrically calibrated sensor. Very fast changing phenomena are of interest; including missile exhaust plumes, missile intercept events, and lightning strikes, hypervelocity impacts, etc. Present sensor capabilities are limited to imaging sensors (producing spatial image), spectrometers (that produce a mean signature over an entire field of view with no spatial resolution), radiometers (producing in-band radiance over an entire FOV), or imaging spectrometers (or hyperspectral sensors, tunable filter type, pushbroom scanning, imaging Fourier Transform, Fabry-Perot, or CTHIS type) that produce a data cube containing spatial/spectral information but suffer from the fact that the cube acquisition process may take longer time than the temporal scale during which the event changes. The Computer Tomography Imaging Spectrometer (CTIS) is another sensor capable of 4D data collection. However, the inversion process for CTIS is computationally extensive and data processing time may be an issue in real-time applications. Hence, the 4D-IS concept with its ability to capture a full image cube at a single exposure and provide real time data processing offers a new and enhanced capability over present sensors.

The 4D-IS uses a reformatter fiber optics to map a 2D image to a linear array that serves as an input slit to an imaging spectrometer. The paper describes three such instruments, a VNIR, a MWIR, and a dual band MW/LWIR. The paper describes the sensors' architecture, mapping, calibration procedures, and remapping the FPA plane into an image cube. Real-time remapping software is used to aid the operator in alignment of the sensor is described. Sample data are shown for rocket motor firings and other events.

**Keywords:** Imaging Spectroscopy, fast events, temporal, spectral, spatial, high speed, Chalcogenide, IR fiberoptics, dual band FPA, Offner spectrograph, mapping

## 1. INTRODUCTION

Certain natural or man-induced events occur on a very short time scale. When the need arises to fully characterize such events across the EO/IR spectral range in the 2D spatial, spectral, and temporal domains, no appropriate sensors are available. The fundamental issue is that EO/IR sensors may use a single element detector, a linear array, or a two-dimensional array of detectors. A single element can capture time dependent signal that at a narrow or broad spectral range. A 1D (linear) array can capture time dependent spatial information (when placed behind imaging optics), or spectral information (when placed in a spectrometer). The 2D matrix array (e.g., CCD, IRFPA) can capture full spatial images at rates that depends on the electronics design of

the sensor (e.g., high speed camera), or spatial-spectral data (e.g., pushbroom hyperspectral sensor), or band sequential images (e.g., in a tunable filter<sup>1</sup> based sensor).

Thus the architecture of EO/IR detectors, containing at most 2D matrix of pixels, limits the information contents that can be captured. If 2D spatial, spectral, and temporal data are needed, there must be a way to “fold” the entire volume of information (2D spatial + spectral at one instant) onto such 2D array.

The 4D-IS sensor sacrifices spatial resolution but maintains high spectral resolution. The fundamental concept of the 4D-IS is shown in Fig. 1. The fore-optics forms an image onto an organized bundle of fiber optics cables. In the cable, the fibers are rearranged from the bundle into a single column. The column of fibers then forms the input slit into an imaging spectrograph (e.g., Offner) that uses a 2D array type detector (FPA). The length of the input slit is roughly equal to the length of the FPA (this dimension of the FPA is called “spatial”). In a perfect world, each fiber in the column is placed vis-à-vis a row of pixels (called “spectral” dimension) onto which the spectrometer disperses the transmitted radiation. Thus, a single snap shot of the camera produces the spectrally dispersed radiation of each spatial fiber.

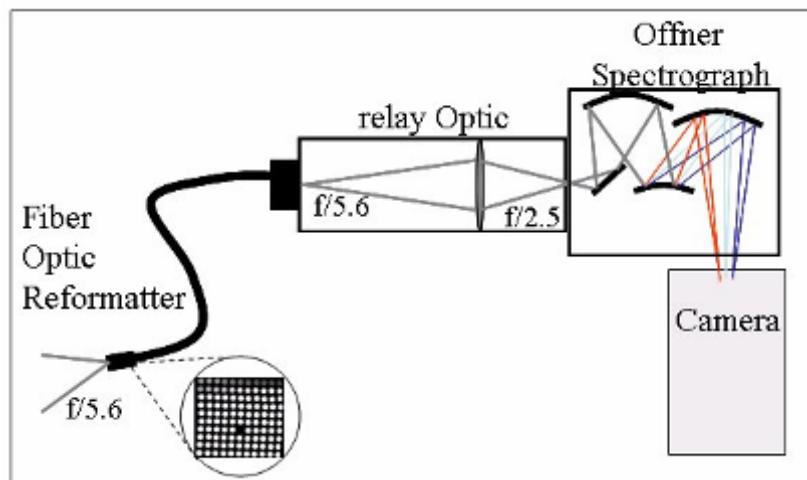


Figure 1. 4D-IS conceptual construction.

In the reconstruction step, the data collected off the FPA must be remapped back to the two-dimensional side of the fiber bundle. The process is illustrated in Figs. 2 and 3.

---

<sup>1</sup> Gat, N. "Imaging Spectroscopy Using Tunable Filters: A Review." Proc. SPIE Vol. 4056, p. 50-64, Wavelet Applications VII, Harold H. Szu, Martin Vetterli; William J. Campbell,, James R. Buss, Ed. (Invited paper). Publ. Date: 04/2000.

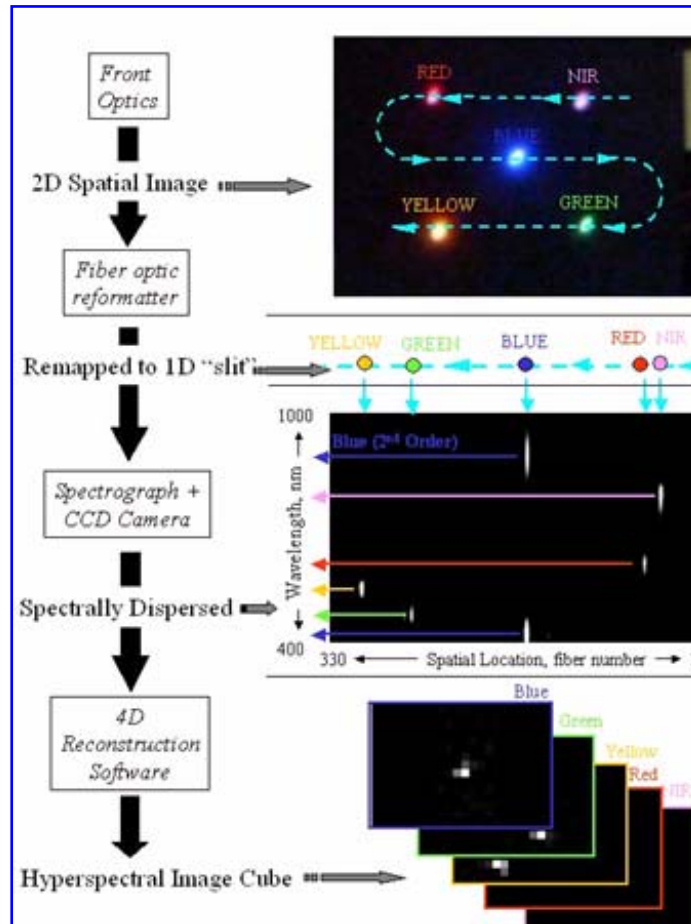


Figure 2. A scene with 5 color LEDs (top) is imaged onto the 2D end, and the image is “unwrapped” into a line; each point source is then dispersed in the imaging spectrometer (center) onto the FPA. A hyperspectral image cube is produced during reconstruction (bottom).

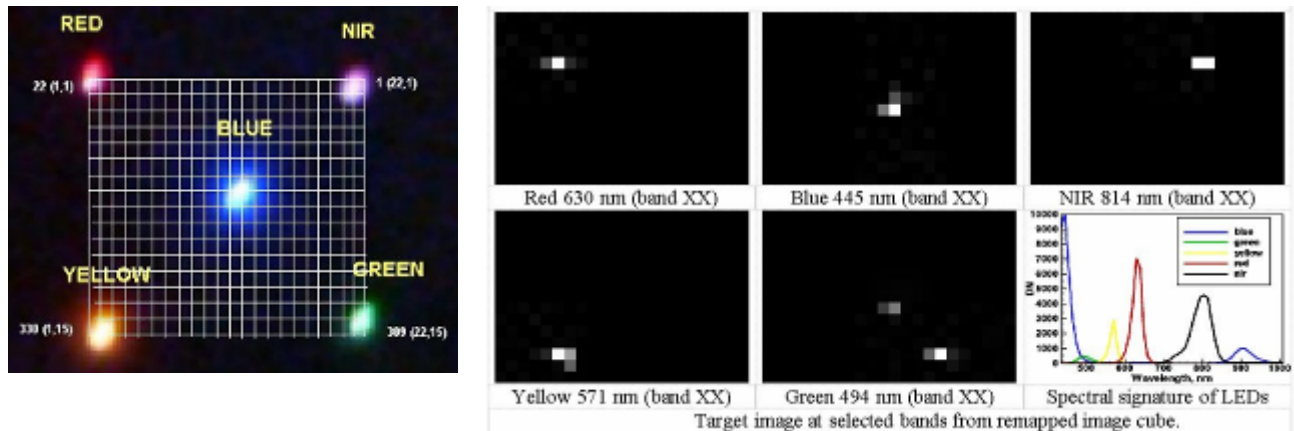


Figure 3. A target with 5 LEDs (left), and 5 images from a hyperspectral cube each showing one of the colored light sources (right); the spectral signature of the LEDs.

## 2. FIBER OPTICS REFORMATTER

Two types of reformatters were developed over time in which various manufacturing techniques were tested for producing optimal reformatter. Silicon glass fibers are used for the VNIR

spectral range, and an early version using a  $22 \times 15$  2D grid with a total of 330 (1D end)  $50 \mu\text{m}$  diameter fibers reformatter is shown in Fig. 2. The image shows several dead or low transmitting fibers.

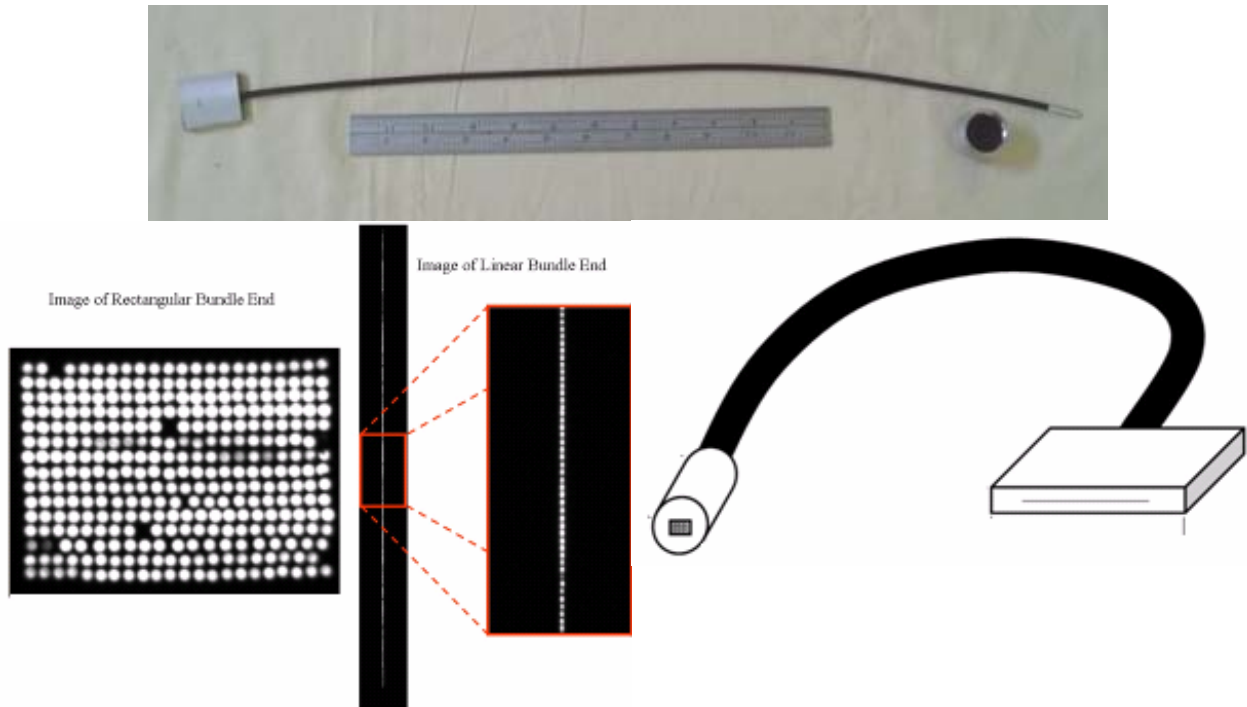


Figure 4. Silica fibers flexible reformatter (top), a magnified image of the 2D and (partial) 1D ends of the reformatter (bottom left), and a schematic showing the reformatter structure.

A  $16 \times 16$ , total of 256,  $70 \mu\text{m}$  diameter Chalcogenide fiber reformatter is shown in Fig. 3. The arrangement of the fibers in this case is not perfectly rectilinear, and a few dead fibers can also be seen. The Chalcogenide works from the NIR to the LWIR (roughly  $800 \text{ nm}$  to over  $12 \mu\text{m}$ ). As such, the performance of the reformatter can be tested with CCD cameras using a bright tungsten lamp. When using the Chalcogenide reformatter in the MWIR or LWIR, the entire assembly is cooled to cryogenic temperature, which presents the biggest challenge in building such devices.



Figure 5. Chalcogenide rigid reformatter (top left), showing the 2D and partial 1D ends.

### 3. SENSORS SPECIFICATIONS

Several 4D-IS type sensors were built and utilized over the past few years. These are listed in Table 1 along with some characteristics. The sensors are shown in Figs. 6 thru 8.

Table 1. 4D-IS sensors characteristics.

	VNIR	MWIR	MW/LWIR
Nominal Spectral Range	400 to 1,000 nm	1.9 to 5.0	3 to 5 (2 <sup>nd</sup> order) & 6 to 10 (1 <sup>st</sup> order)
FPA type, res & pixel size	CCD or CMOS (used with different cameras as needed)	InSb, 640×512, 25 μm (SBFP)	Dual Band MCT, 256×256, 30 μm (Raytheon)
Dispersion / pixel	1.2 nm	5 nm	15 nm MW; 7 nm LW
Spectral resolution	10 nm with binning	~10 nm	30 nm MW / 15 nm LW
Min exposure time	~ μsec	~1 μsec	< 1 msec
Reformatter	Silica	Chalcogenide	Chalcogenide
Frame rate	Up to 190,000 fps depending on camera and windowing	Up to 84 fps with windowing	33 fps
Cooling & operating temp.	None (TE for some CCDs)	Two 5W Stirling for optical bench & rad shield down to 150K, a 1W Stirling for FPA to 77K	LN2 for optical bench & rad shield to 77K, 1W Stirling for FPA to 66K
Spectrograph	Offner	Offner, Aluminum optics and bench	
Vacuum	No	~ 10 <sup>-6</sup> torr	



Figure 6. MW/LWIR 4D-IS sensor: actual system (left), 3D CAD model (right), showing the maintenance LN2 dewar in the back, which allows the sensor to run for several hours without connection to a large LN2 tank. The sensor is mounted on a custom designed plate that fits on standard KTM tracker mounts.



Figure 7. MWIR 4D-IS: actual sensor (left) with a bore-sighted Phantom and wide FOV tracking cameras on top, and a 3D CAD with the radiation shield removed (right). The sensor is designed for airborne operations and is cooled with Stirling cryo-coolers.

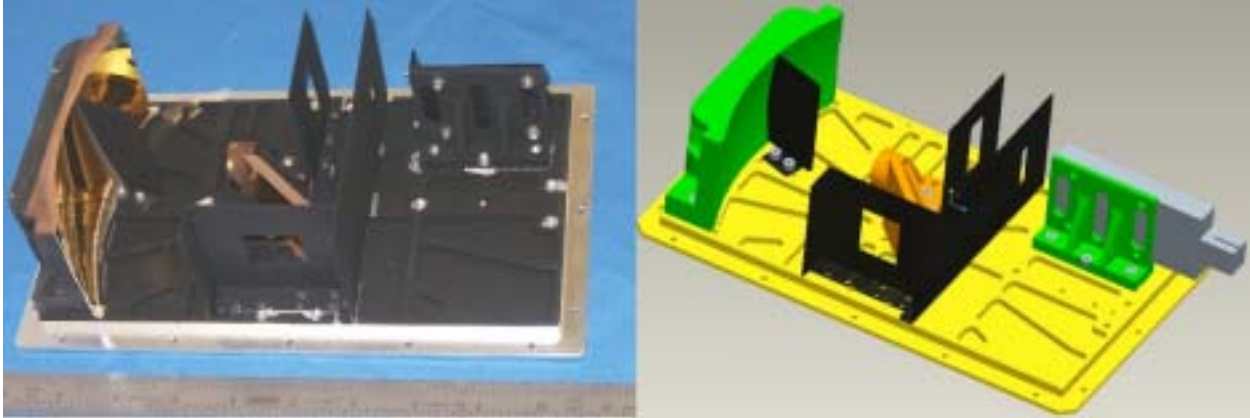


Figure 8. MWIR 4D-IS, showing the stray-light baffles, and primary / tertiary Offner mirror, grating, turning flat, and rigid reformatter are all mounted to the optical bench that is cooled to 150K.

#### 4. ALIGNMENT & CALIBRATION

All sensors must undergo a sequence of alignment, mapping, and spectral and radiometric calibration. Since each fiber transmission may be slightly different, and since pixel response may also be different, the sensor is mapped and calibrated once it is assembled.

##### 4.1 Mapping

The mapping process creates a spatial relationship in the object space to the FPA. This is done by translating a pinhole source (typically a pinhole mounted on a motorized X-Y stage, moving in front of a blackbody source) and registering the FPA response. One pinhole position may register over one or more row of pixels on the FPA. The mapping is used for the reconstruction of object images from the data captured on the FPA.

##### 4.2 Calibration

The spectral calibration is accomplished using narrow spectral sources (e.g., Hg, Ar, HeNe sources) for the VNIR sensor, and cold narrow band pass filters for the IR systems. A cold filter wheel is built into the sensors. Once the spectral calibration is established, the radiometric calibration can be accomplished. Radiometric calibration is performed with a NIST traceable tungsten-halogen lamp, for the VNIR sensor, and with a 1000°C blackbody source for the IR sensors.

For the radiometric calibration, the black body is collimated using 8" Off Axis Parabolic Collimator. The Optics of the 4D-IS is focused to infinity. N<sub>2</sub> purge is used to remove CO<sub>2</sub> and H<sub>2</sub>O in the intervening atmosphere, so that the calibration can be obtained over the entire spectral range (and not suffer from the 2.7μm (water) and 4.3μm (carbon dioxide) and other weaker absorption bands, Fig. 9.

The mapping/remapping process and the calibration allow for the reconstruction of images.

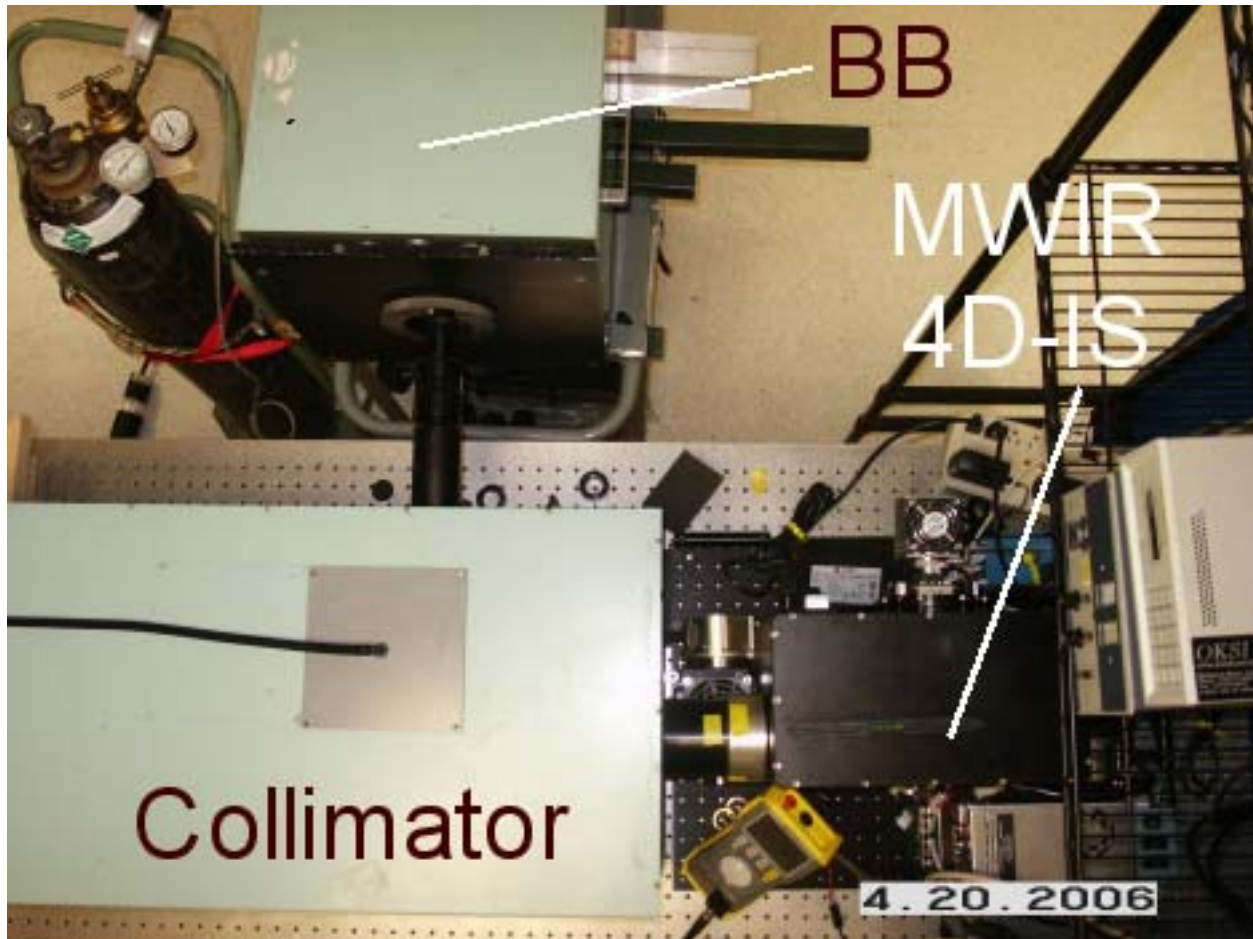


Figure 9. MWIR 4D-IS calibration using a 2" aperture, 1000°C blackbody source, a 8" aperture collimator, and N<sub>2</sub> purge to remove atmospheric absorption.

### 5. SAMPLE MEASUREMENTS

A model rocket engine firing is shown in Fig. 11, along with the FOV of the VNIR 4D-IS. Two plume images at 1 second at the sodium and potassium emission bands are shown in the figure. The full 4-dimensional aspect of this type of measurements is depicted in Figs. 10a and 10b that show several intensity profiles for the plume.

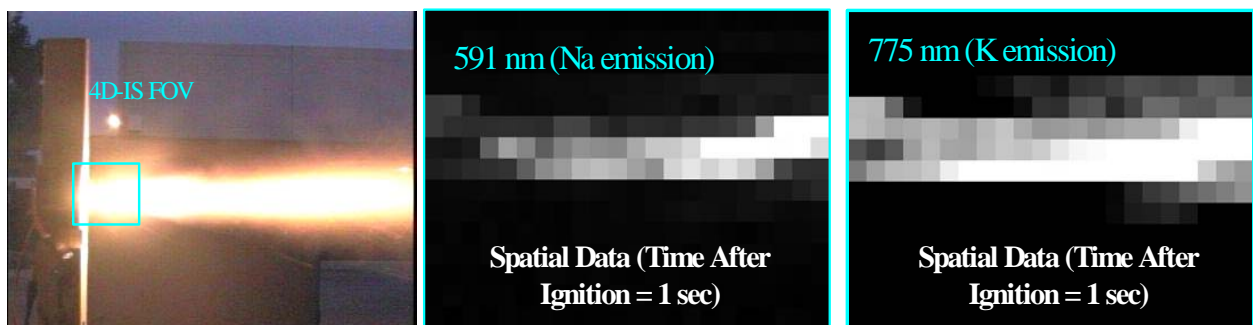


Figure 10. Model rocket engine firing (left) and two images of the plume at the sodium and potassium emission lines.

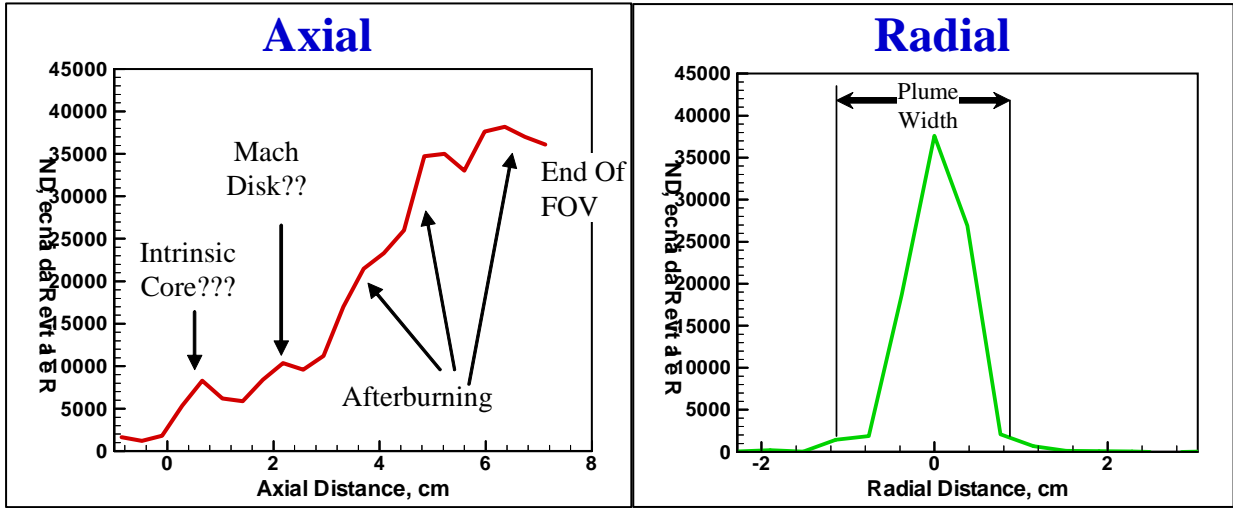


Figure 11a. Axial and radial intensity profiles in the model rocket plume.

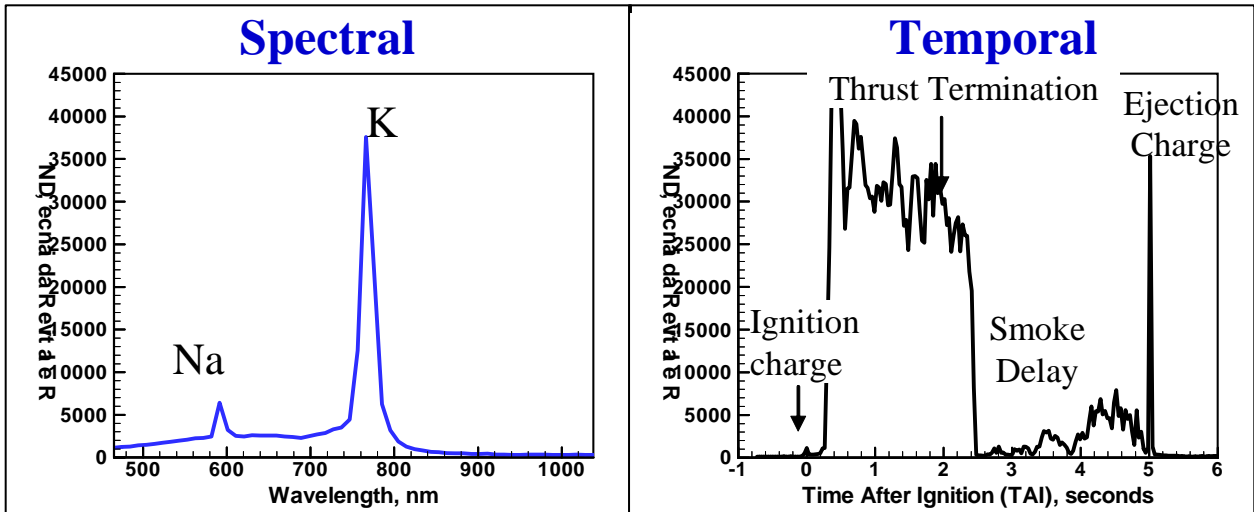


Figure 11b. Spectral and temporal intensity profiles of the model rocket plume.

Another measurement with the VNIR 4D-IS of a very high voltage discharge in air is shown in Fig. 12. This measurement shows the ability to achieve adequate spectral resolution for atomic emission spectroscopy. The various single and doubly ionized species are identified based on the NIST spectral library. A similar measurement in a gas gun shows the emission generated within the first 1 msec following the impact of a hypervelocity projectile onto a target, Fig. 13. Another sample of 4D-IS data is shown in Fig. 14.

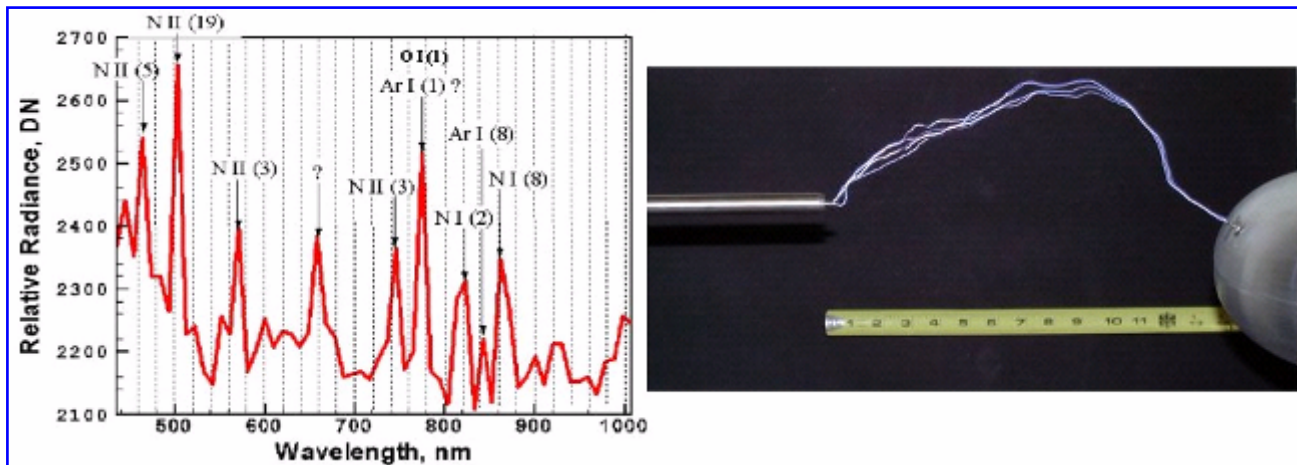


Figure 12. Spectra of ionized air (left) produced by a 250 KV Tesla coil discharge (right).

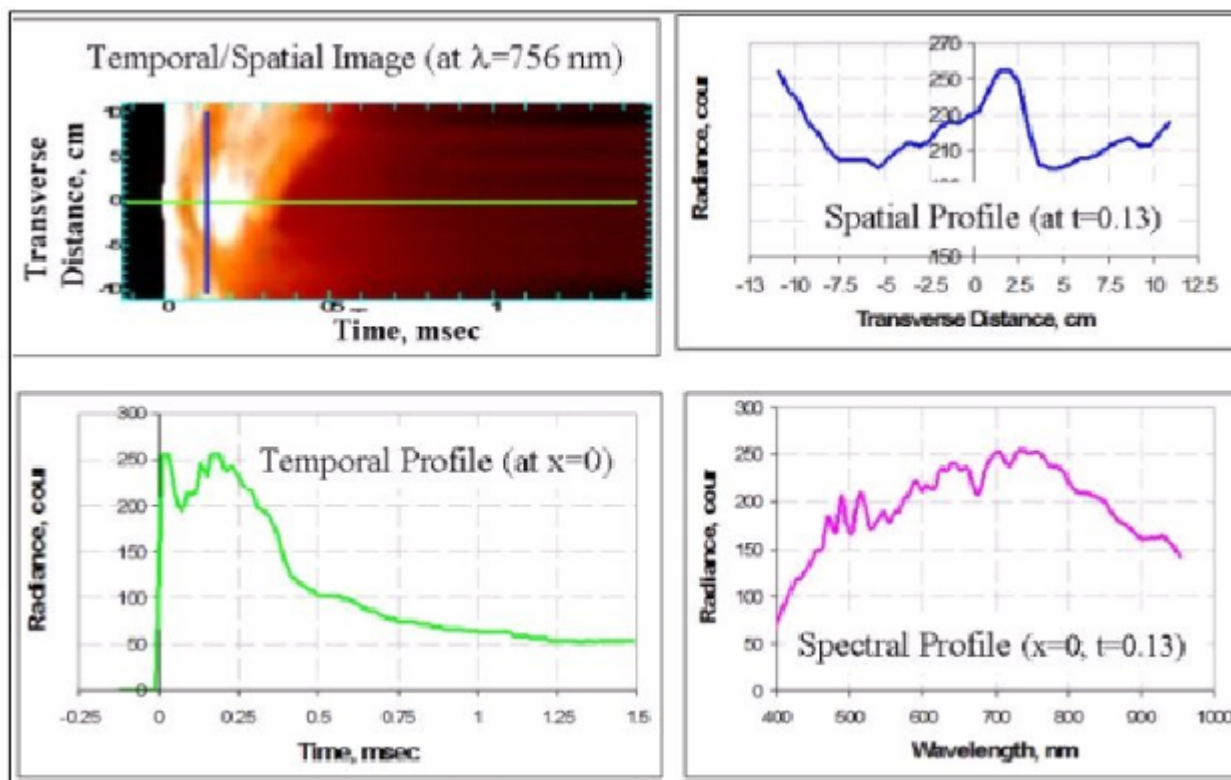


Figure 13. Emission within the first 1 msec following the impact of hypervelocity projectile onto a target. The color scheme in the top left graph goes from black (low intensity, thru red, to white (highest intensity). Several profiles are shown in raw sensor counts.

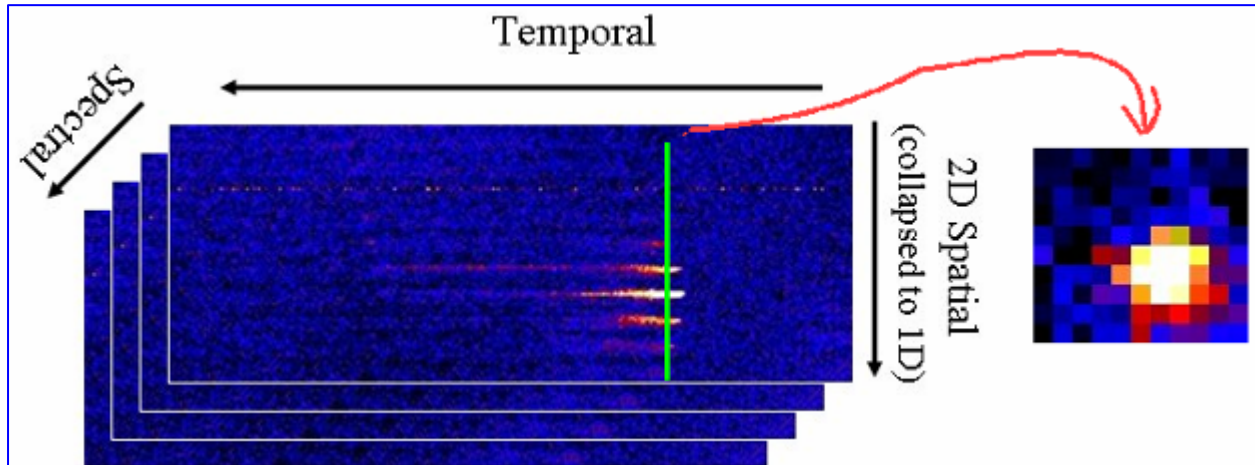


Figure 14. 4D-IS data of a high energy impact even over the atmosphere at a range of several hundreds of kilometers, showing spatial, spectral, and temporal data maps, and a sample of a remapped image at one time slice at one wavelength.

## 6. SUMMARY

The 4D-IS concept was developed into field deployable sensors covering the VNIR, MWIR and a dual band MW/LWIR. These sensors operate at a relatively low spatial resolution but produce high spectral and temporal resolution. The development entailed complete optical design, vacuum and cryocooling system, mechanical design, software for sensor operation and data capture, alignment, spectral and radiometric calibration, and software for the remapping (unwrapping) of the data into image cubes.

The paper shows several examples of measurements of fast changing events. In such events, several sensors would be needed to capture the full extent of the data and such sensors would have to be well synchronized in order to capture the true nature of the phenomenology. The 4D-IS provides a single sensor substitute for the collection of other sensors. Examples of 4D-IS applications include missile plume phenomenology, gas gun impact tests, kill assessment during missile defense intercept events, and lightning characterization. Newer versions of some of the sensors and expanded spectral range sensors are presently under development.